

# Dielectrophoresis and electrohydrodynamics-mediated fluidic assembly of silicon resistors

S. W. Lee and R. Bashir<sup>a)</sup>

Laboratory of Integrated Biomedical Micro/Nanotechnology, Birck Nanotechnology Center, School of Electrical and Computer Engineering, Department of Biomedical Engineering, Purdue University, West Lafayette, Indiana 47907

(Received 19 June 2003; accepted 17 September 2003)

In this letter, we present techniques, utilizing dielectrophoresis and electrohydrodynamics, which can be used for assembling single-crystal silicon devices suspended in a solution onto a binding site on a heterogeneous substrate. Silicon resistors with gold/chromium layers located at the end of the resistors and silicon blocks without metal were fabricated on bonded and etched-backed silicon-on-insulator wafers and successfully released into deionized water. The devices were subsequently assembled on a different substrate at specific binding sites by dielectrophoretic and electrohydrodynamic forces with submicron precision. Current–voltage measurements of the assembled resistors exhibited low contact resistance after the solution was completely evaporated and the contacts were annealed. © 2003 American Institute of Physics. [DOI: 10.1063/1.1624642]

An object in a solution under nonuniform electric field is polarized, resulting in a dipole moment. Due to the interactions between the dipole moment and electric field, the device is moved in the solution. This phenomenon is called dielectrophoresis (DEP), and has been described earlier.<sup>1</sup> Through the use of microfabrication techniques, the application of DEP phenomenon has become more and more important in recent years. For example, dielectrophoretic effect has been used to separate and manipulate cells<sup>2,3</sup> and nanoparticles of different sizes.<sup>4,5</sup> Metallic nanowires have been aligned and assembled on a micro-interdigitated (IDT) electrodes using DEP force.<sup>6</sup> It is also important to note that when a high electric field is applied to these microstructures, power is generated, which causes the generation of heat in a medium, resulting in local temperature gradients. Due to the local temperature gradients, the spatial variations of electrical conductivity and permittivity occur, leading to an electrothermal force.<sup>7,8</sup> This electrothermal force can play an equally important role in the motion of the suspended and polarized devices, when compared to the role of the DEP forces. Fluidic assembly of  $\sim 100\ \mu\text{m} \times 100\ \mu\text{m} \times 50\ \mu\text{m}$  silicon blocks with transistors has been achieved using gravitational forces and shape-mediated effects,<sup>9</sup> but as the device size is made smaller, these forces cannot be used alone, and “directed” assembly is required. In this letter, we demonstrate that silicon resistors and blocks (less than  $10\ \mu\text{m}$  on a side) suspended in a solution are positioned and assembled onto a target circuitry. Moreover,  $I$ – $V$  characteristic of the assembled resistors is also reported after the solution was evaporated completely. This work lays the foundation of using three-terminal transistors with directed fluidic self-assembly.

The fabrication of the silicon resistors is shown in Figs. 1(a)–1(d), and began on a commercially available bonded and etched silicon-on-insulator (BESOI) wafer, having a  $2.5\text{-}\mu\text{m}$  ( $\pm 0.5\ \mu\text{m}$ )-thick top silicon layer and a  $1\text{-}\mu\text{m}$ -thick

buried oxide layer.<sup>10</sup> The SOI layer thickness was reduced to  $1.4\ \mu\text{m}$  by thermal oxidation and etching. Subsequently, the top silicon layer was heavily doped with phosphorus using a spin-on-glass source. Thermal dioxide with thickness of  $0.15\ \mu\text{m}$  was grown and patterned to define the size of the resistor. The silicon layer was etched at a temperature of  $55\ ^\circ\text{C}$  for 12 min in a solution consisting of 30 g of KOH, 250 ml of deionized (DI) water, and 80 ml of 2-propanol, using the oxide as a mask, as shown in Fig. 1(a). Photolithography techniques were used to define  $4\ \mu\text{m} \times 6\ \mu\text{m}$  windows in a photoresist mask for subsequent lift-off of metal. A  $150\text{-}\text{\AA}$ -thick chromium layer and a  $500\text{-}\text{\AA}$ -thick gold layer were deposited sequentially in an electron-beam evaporator and patterned using the lift-off process, as shown in Fig. 1(b). The wafer was then placed in hydrofluoric acid solution to partially etch buried oxide, while leaving pedestals holding the silicon resistor on the substrate, as shown in Fig. 1(c). The substrate was then immersed in DI water with 0.05% Tween-20 and the silicon resistors were released in an ultra-

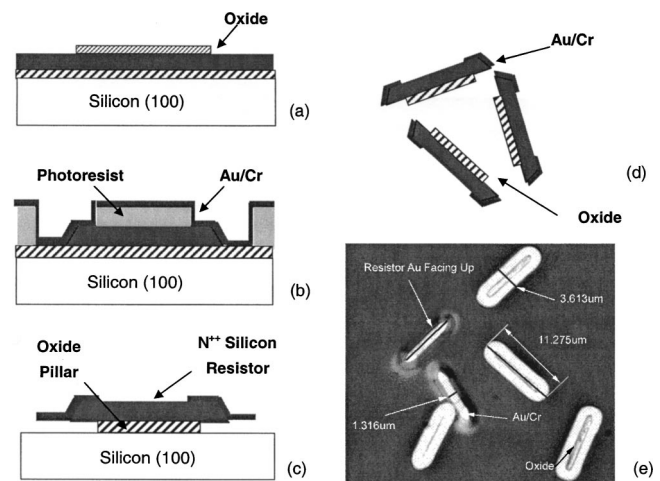


FIG. 1. (a)–(d) Fabrication process for building silicon resistors and releasing the resistors from a BESOI wafer to DI water with 0.05% Tween-20. (e) Optical micrographs of the released resistors on a chip surface.

<sup>a)</sup>Electronic mail: bashir@ecn.purdue.edu

sonic agitator at a frequency of 40 KHz. The oxide pedestal holding the islands to the substrates broke off, thus releasing the islands in the DI water, as shown in Fig. 1(d). Figure 1(e) shows the released silicon resistors in an optical micrograph with 1000 $\times$  magnification. The fabrication of silicon blocks was similar to the process just described, except that no spin-on dopant process was done, a photoresist mask with 4  $\mu\text{m} \times 4 \mu\text{m}$  was used for reactive ion etching of silicon to produce blocks with vertical sidewalls, and no metal films were deposited on these blocks. A 50  $\mu\text{l}$  solution containing the silicon resistors or the silicon blocks was introduced onto the IDT electrodes, and examined under a microscope. A sinusoidal signal with 10 V and 10 MHz was applied using micromanipulator probes, while a silicone rubber ring isolated the probes from the solution at the test sites. An HP 4156A was used for measuring the  $I$ - $V$  curve of the assembled device on microelectrodes after the solution was completely evaporated. The movement of devices was recorded using a CCD camera.

The Clausius-Mossotti (CM) factor in the DEP force equation is given by the following formula:  $\text{Re}[K(\omega)] = \text{Re}[(\tilde{\epsilon}_p - \tilde{\epsilon}_m)/(\tilde{\epsilon}_p + 2\tilde{\epsilon}_m)]$ , where  $\tilde{\epsilon}_p$  and  $\tilde{\epsilon}_m$  are complex permittivities of a suspended object and a medium, respectively. When the CM factor is positive, DEP force acts on a particle to move it towards the region of the largest field gradient. However, the particle moves toward the region where the field gradient is smallest when the CM factor is negative. For the silicon blocks of  $4 \times 4 \times 1.4 \mu\text{m}^3$  (conductivity and permittivity of silicon block  $\approx 0.0025$ – $0.01$  S/m, and  $11.9\epsilon_0$ , respectively, conductivity and permittivity of DI buffer =  $10^{-6}$  S/m and  $80\epsilon_0$ , respectively), the CM factor becomes positive at low frequencies and becomes negative at high frequencies. Thus, the negative DEP force acts on the blocks to move toward the center of the IDT electrode at 10 MHz, where the gradient of the ac field is the smallest,<sup>3,11</sup> as shown in Fig. 2(a). However, the phenomenon that the blocks are located between the open windows cannot be explained if only negative DEP exists in the system. This fact can be explained by considering electrothermal effects, since near the exposed window, power is generated by the current flowing between the electrodes. The generated power leads to a local temperature gradient, causing the gradients of conductivity and permittivity of the medium. As a result, a fluidic motion is created where the direction of this fluid is expected to be, as shown in Fig. 2(b); that is, starting from the edge of the exposed windows on the electrode, flowing parallel to the width of the windows, converging at the center of the windows, and then moving upwards.<sup>3,5</sup> The fact that the blocks were positioned vertically provides verification of fluidic direction generated by electrothermal force since the vertical placement of the blocks is the favorable position in steady state. The motion of suspended silicon resistors with Au/Cr films as shown in Fig. 2(c) is dictated by positive DEP effects since the conductivity of the films (Au  $\approx 4 \times 10^7$  S/m and Cr  $\approx 7 \times 10^6$  S/m) on the resistors results in a positive CM factor. Thus, resistors align between the exposed metal openings between two electrodes, as shown in Fig. 2(c).

The assembly of the silicon resistor between two electrodes is shown in Fig. 3. The resistors were distributed randomly in the solution before voltage was applied. As shown

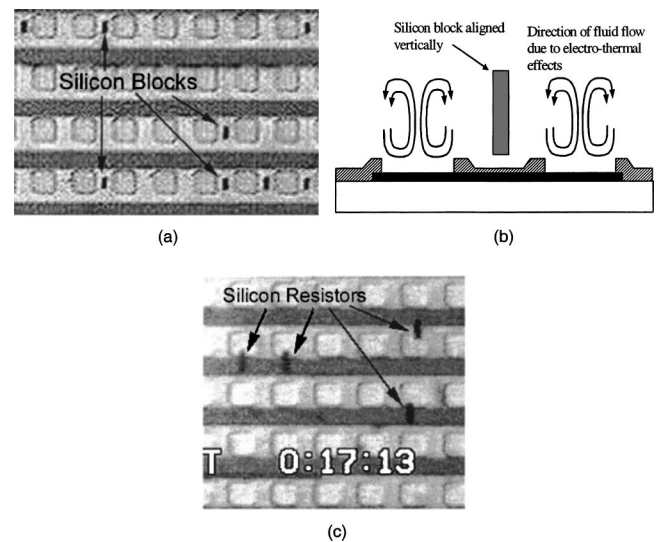


FIG. 2. Negative DEP electrothermal effects and positive DEP effects in silicon blocks and resistors with metal contacts. (a) Optical micrograph of the silicon blocks taken 5 min after 10 V at 10 MHz was applied. Silicon blocks are arranged vertically on the oxide in between the open windows due to negative DEP. (b) Schematic of the fluid flow lines due to electrothermal effects and the alignment of the silicon blocks in between the oxide [as observed in Fig. 2(a)]. (c) 1 min 50 s after 10 V at 10 MHz was applied, and the resistors move between the contact openings across two adjacent metal electrodes due to positive DEP.

in Fig. 3(a) and in the magnified inset, when an ac signal with 10 V and 10 MHz was applied, the resistor moved to the region having the largest gradient of the ac field and was assembled in between the Au/Cr electrodes. If the voltage was turned off, the resistor was seen to move away from the assembly site in the solution, as shown in Fig. 3(b). The resistor can be re-aligned after the signal was applied, as shown Fig. 3(c). The solution was allowed to evaporate while the ac signal was still applied into the electrode. This process ensured that the resistor stayed at the original posi-

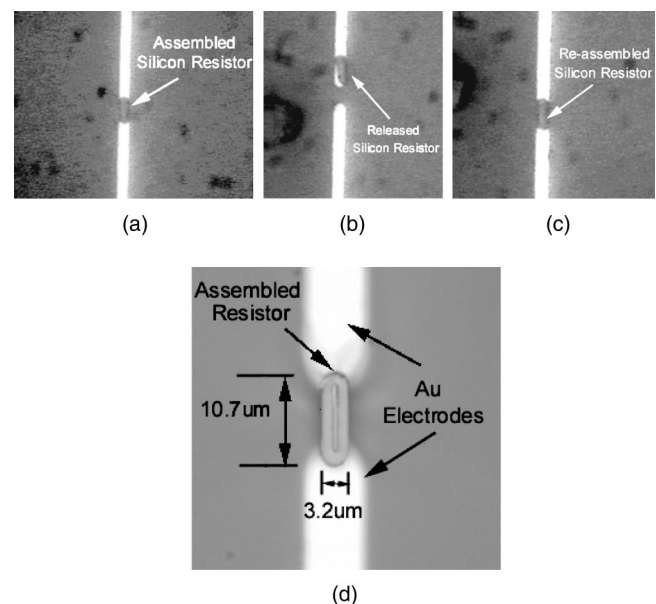


FIG. 3. Self-assembly of a silicon resistor using positive DEP. (a) Optical micrograph of the assembled resistor 1 min 30 s after the signal was applied, (b) 11 min after the signal turned off, and (c) 3 min after the signal was re-applied into the system. (d) Close-up of the assembled resistors after the solution is dried.

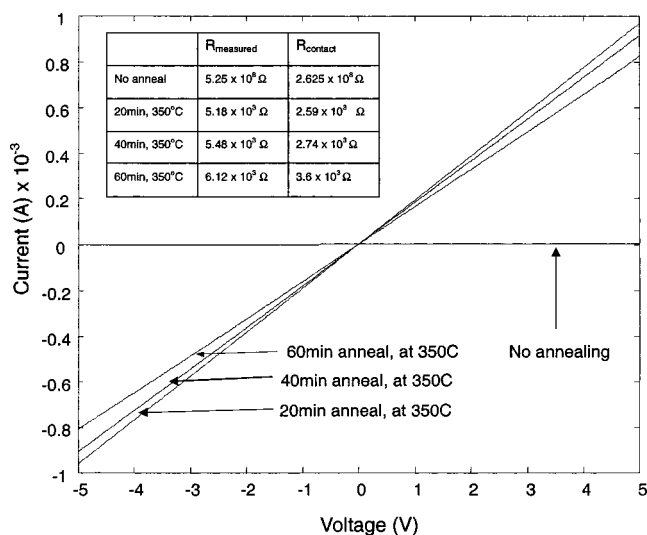


FIG. 4.  $I$ - $V$  characteristics of the assembled resistor, measured after the evaporation was completed, and annealed at 350 °C for various times.

tion upon drying.  $I$ - $V$  measurement of the assembled resistor was performed as shown in Fig. 4. The assembled devices showed no current due to a high contact resistance between the Au electrodes on the devices and the Au electrodes on the substrate. When the devices were annealed in air at 350 °C, current flow can be measured through the device. The current actually drops slightly with increase in annealing time. The contact resistance of the resistor can be calculated using the following formula:  $R_{\text{measured}} = R_{\text{silicon}} + 2R_{\text{contact}}$ , where  $R_{\text{silicon}} = 6.39 \times 10^{-4} \Omega$  extracted using four-point probe method and calculated using the dimensions. The contact resistance as function of annealing time is summarized in the inset in Fig. 4.

In summary, self-assembly of silicon resistors and blocks on microelectrode structures by dielectrophoretic and elec-

trohydrodynamic effects was demonstrated and explained. We demonstrated that the silicon resistor with Au contacts can be assembled precisely within two electrodes and the devices can be held at the same position during the evaporation process. Moreover, the assembled process in solution can be reversible.  $I$ - $V$  characteristics of the assembled device were measured on devices after drying and annealing the contacts. DEP and electrohydrodynamics mediated self assembly described in this letter can be used for heterogeneous integration of micro- and nanoelectronic devices for flexible displays and electronics, power electronics, and microelectro mechanical systems applications.

The authors would like to acknowledge the support NSF ITR grant 0135946-EIA for funding the work and for support (S.W.L.). The authors would also like to thank Rafael Gomez, Amit Gupta, Haibo Li, Dr. Helen McNally, Dr. Woo-Jin, and Prof. Don Bergstrom for valuable discussions. The authors would also like to thank the staff of the microfabrication facilities at Birck Nanotechnology Center at Purdue University for wafer processing.

<sup>1</sup>H. A. Pohl, *Dielectrophoresis* (Cambridge University Press, Cambridge, UK, 1978).

<sup>2</sup>X. Wang, Y. Huang, P. Gascoyne, and F. F. Becker, *IEEE Trans. Ind. Appl.* **33**, 660 (1997).

<sup>3</sup>H. Li and R. Bashir, *Sens. Actuators B* **36**, 1 (2002).

<sup>4</sup>N. G. Green and H. Morgan, *J. Phys. D* **30**, L41 (1997).

<sup>5</sup>N. G. Green and H. Morgan, *J. Phys. D* **31**, L25 (1998).

<sup>6</sup>P. A. Smith, C. D. Nordquist, T. N. Jackson, and T. S. Mayer, *Appl. Phys. Lett.* **77**, 1399 (2000).

<sup>7</sup>A. Ramos, H. Morgan, N. G. Green, and A. Castellanos, *J. Phys. D* **31**, 2338 (1998).

<sup>8</sup>A. Ramos, H. Morgan, N. G. Green, and A. Castellanos, *J. Electrostat.* **47**, 71 (1999).

<sup>9</sup>J. S. Smith, *Tech. Dig. - Int. Electron Devices Meet.*, 201 (2000).

<sup>10</sup>S. W. Lee, H. A. McNally, D. Guo, M. Pingle, D. E. Bergstrom, and R. Bashir, *Langmuir* **18**, 3383 (2002).

<sup>11</sup>X. Wang, F. F. Becket, and P. R. C. Gascoyne, *J. Phys. D* **29**, 1649 (1996).